

Supporting Information

N-heterocyclic carbene adducts of the heavier group 15 tribromides. Normal to abnormal isomerism and bromide ion abstraction.

*Jordan B. Waters, Qien Chen, Thomas A. Everitt and Jose M. Goicoechea**

Department of Chemistry, University of Oxford, Chemistry Research Laboratory,
12 Mansfield Road, Oxford, OX1 3TA, U.K.

E-mail: jose.goicoechea@chem.ox.ac.uk

CONTENTS:

- 1. Single crystal X-ray diffraction data**
- 2. NMR spectra**
- 3. ESI-MS spectra**
- 4. Computational details**

1. Single crystal X-ray diffraction data

	[1]·2THF	[2]·0.5THF	[3][AlBr ₄]·0.5DCM	[4][AlBr ₄]·0.5DCM
Formula	C ₃₅ H ₅₂ Br ₃ N ₂ O ₂ Sb	C ₂₉ H ₄₀ BiBr ₃ N ₂ O _{0.5}	C _{27.5} H ₃₇ AlBr ₆ ClN ₂ Sb	C _{27.5} H ₃₇ AlBiBr ₆ ClN ₂
Fw [g mol ⁻¹]	894.26	873.34	1059.23	1146.46
Crystal system	Monoclinic	Monoclinic	Triclinic	Triclinic
Space group	P2 ₁ /n	P2 ₁ /c	PError!	PError!
a (Å)	12.9636(3)	35.3941(3)	12.2078(3)	12.2474(3)
b (Å)	20.2935(4)	17.9516(1)	17.4963(3)	17.4318(6)
c (Å)	14.3419(3)	20.0953(2)	18.3277(4)	18.3406(6)
α (°)	90	90	76.528(2)	77.136(2)
β (°)	96.532(2)	95.253(1)	79.988(2)	79.952(2)
γ (°)	90	90	81.945(2)	82.507(2)
V (Å ³)	3748.53(14)	12714.54(18)	3728.61(14)	3741.60(20)
Z	4	16	4	4
Radiation, λ (Å)	Cu Kα, 1.54184	Cu Kα, 1.54184	Cu Kα, 1.54184	Cu Kα, 1.54184
ρ _{calc} (g cm ⁻³)	1.585	1.825	1.887	2.035
μ (mm ⁻¹)	9.821	15.457	14.440	17.789
Reflections collected	75905	202772	50023	41661
Independent reflections	7831	26537	15405	15503
Parameters	462	1293	694	679
R(int)	0.0673	0.0714	0.0410	0.0325
R1/wR2, ^[a] I ≥ 2σI (%)	4.66/12.07	4.86/12.54	4.04/10.54	3.99/10.38
R1/wR2, ^[a] all data (%)	5.07/12.62	5.07/12.73	4.31/11.00	4.09/10.48
GOF	1.046	1.108	1.058	1.058

^[a] R1 = $[\sum|F_o - |F_c||]/\sum|F_o|$; wR2 = $\{[\sum w[(F_o)^2 - (F_c)^2]^2]/[\sum w(F_o)^2]\}^{1/2}$; w = $[\sigma^2(F_o)^2 + (AP)^2 + BP]^{-1}$, where P = $[(F_o)^2 + 2(F_c)^2]/3$ and the A and B values are 0.0678 and 9.31 for [1]·2THF, 0.0589 and 167.06 for [2]·0.5THF, 0.0644 and 15.87 for [3][AlBr₄]·0.5DCM and 0.0620 and 16.80 for [4][AlBr₄]·0.5DCM.

	[5]·2THF	[6]·2THF	[6]·0.5DCM	[7][BAr ^F ₄]·4THF
Formula	C ₃₅ H ₅₂ Br ₃ N ₂ O ₂ Sb	C ₃₅ H ₅₂ BiBr ₃ N ₂ O ₂	C _{27.5} H ₃₇ BiBr ₃ ClN ₂	C ₇₅ H ₈₀ BBr ₂ F ₂₄ N ₂ O ₄ Sb
Fw [g mol ⁻¹]	894.26	981.49	879.75	1821.79
Crystal system	Triclinic	Triclinic	Monoclinic	Triclinic
Space group	<i>P</i> Error!	<i>P</i> Error!	<i>P</i> 2 ₁ /c	<i>P</i> Error!
<i>a</i> (Å)	11.8063(3)	11.105(2)	12.1007(2)	13.2348(2)
<i>b</i> (Å)	11.8231(2)	11.908(2)	35.0892(5)	16.9730(4)
<i>c</i> (Å)	15.2363(3)	15.263(3)	14.9693(2)	18.9206(4)
α (°)	98.938(2)	98.77(3)	90	72.072(2)
β (°)	101.958(2)	102.17(3)	98.858(1)	83.509(2)
γ (°)	95.680(2)	96.09(3)	90	87.014(2)
<i>V</i> (Å ³)	1912.17(7)	1929.7(7)	6280.21(16)	4017.25(15)
<i>Z</i>	2	2	8	2
Radiation, λ (Å)	Cu K α , 1.54184	Mo K α , 0.71703	Cu K α , 1.54184	Cu K α , 1.54184
ρ_{calc} (g cm ⁻³)	1.553	1.689	1.861	1.506
μ (mm ⁻¹)	9.626	7.705	16.405	4.802
Reflections collected	38814	31667	78548	81697
Independent reflections	7943	6703	13121	16691
Parameters	426	426	622	1092
R(int)	0.0402	0.0357	0.0549	0.0541
R1/wR2, ^[a] I $\geq 2\sigma$ I (%)	4.30/11.05	4.63/12.09	5.34/13.85	5.84/15.70
R1/wR2, ^[a] all data (%)	4.60/11.44	5.52/12.63	5.36/13.87	6.22/16.15
GOF	1.045	1.052	1.172	1.049

^[a] R1 = $[\Sigma ||F_o| - |F_c||]/\Sigma |F_o|$; wR2 = $\{\sum w[(F_o)^2 - (F_c)^2]^2\}/[\sum w(F_o^2)^2\}^{1/2}$; w = $[\sigma^2(F_o)^2 + (AP)^2 + BP]^{-1}$, where P = $[(F_o)^2 + 2(F_c)^2]/3$ and the A and B values are 0.0584 and 3.77 for [5]·2THF, 0.0751 and 4.26 for [6]·2THF, 0.0781 and 40.31 for [6]·0.5DCM and 0.0816 and 6.85 for [7][BAr^F₄]·4THF.

	[8][BAr ^F ₄]·4.5THF	[9]Br·0.5THF	[9][AlBr ₄]
Formula	C ₇₇ H ₈₄ BBiBr ₂ F ₂₄ N ₂ O _{4.5}	C ₅₆ H ₇₆ Br ₃ N ₄ O _{0.5} Sb	C ₅₄ H ₇₂ AlBr ₆ N ₄ Sb
Fw [g mol ⁻¹]	1945.07	1174.68	1405.34
Crystal system	Triclinic	Monoclinic	Orthorhombic
Space group	<i>P</i> Error!	<i>P</i> 2 ₁ /n	<i>P</i> 2 ₁ 2 ₁ 2 ₁
<i>a</i> (Å)	12.7012(3)	14.8865(2)	10.5273(1)
<i>b</i> (Å)	18.9400(4)	18.9920(2)	18.6503(1)
<i>c</i> (Å)	19.7427(4)	20.8333(2)	30.8129(2)
α (°)	113.243(2)	90	90
β (°)	93.206(2)	98.610(1)	90
γ (°)	106.828(2)	90	90
<i>V</i> (Å ³)	4098.06(17)	5823.70(12)	6049.72(8)
<i>Z</i>	2	4	4
Radiation, λ (Å)	Cu K α , 1.54184	Cu K α , 1.54184	Cu K α , 1.54184
ρ_{calc} (g cm ⁻³)	1.576	1.340	1.543
μ (mm ⁻¹)	6.275	6.445	8.669
Reflections collected	83484	79376	63776
Independent reflections	16981	12155	12555
Parameters	1091	620	611
R(int)	0.0473	0.0359	0.0317
R1/wR2, ^[a] I $\geq 2\sigma$ I (%)	5.67/14.07	3.91/10.28	2.43/5.89
R1/wR2, ^[a] all data (%)	6.33/14.79	4.08/10.49	2.50/5.95
GOF	1.034	1.053	1.023

^[a] R1 = $[\sum|F_o - |F_c||]/\sum|F_o|$; wR2 = $\{[\sum w[(F_o)^2 - (F_c)^2]^2]/[\sum w(F_o^2)^2]\}^{1/2}$; w = $[\sigma^2(F_o)^2 + (AP)^2 + BP]^{-1}$, where P = $[(F_o)^2 + 2(F_c)^2]/3$ and the A and B values are 0.0643 and 14.41 for [8][BAr^F₄]·4.5THF and 0.0569 and 8.14 [9]Br·0.5THF and 0.0255 and 6.33 for [9][AlBr₄].

2. NMR spectra

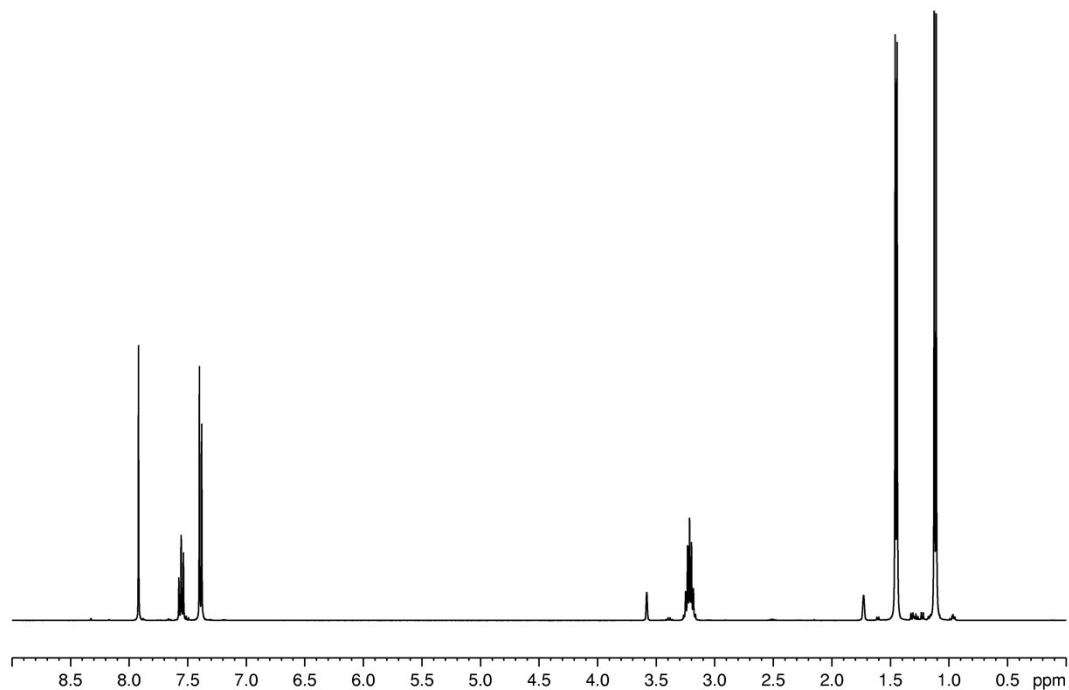


Figure S1. ^1H NMR spectrum of **1** in $d_8\text{-THF}$.

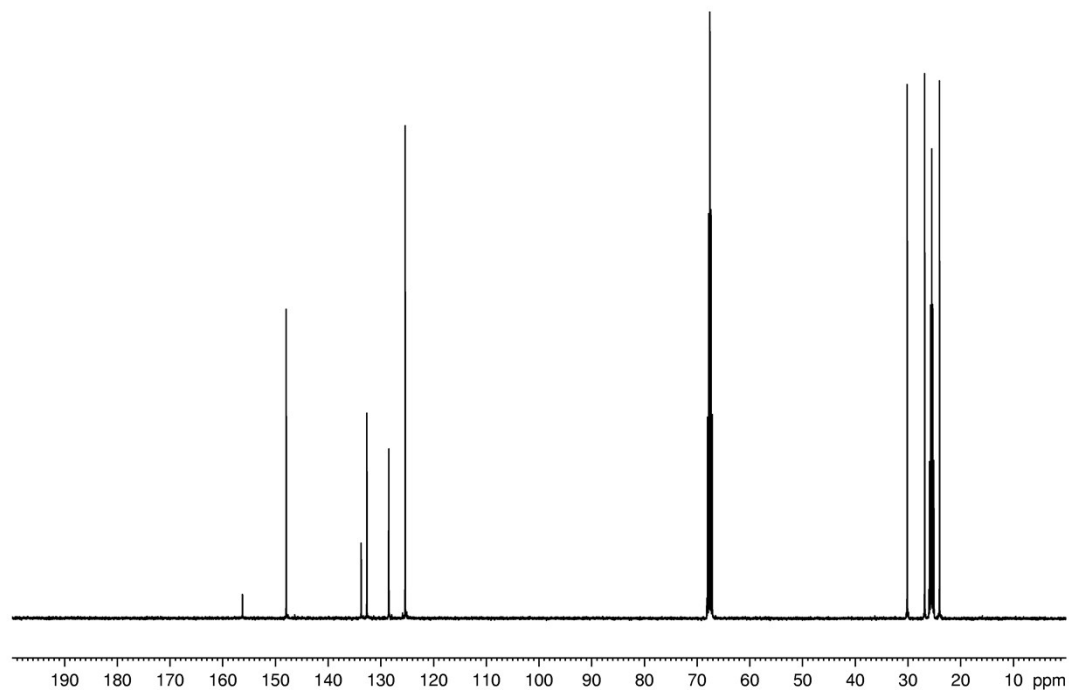


Figure S2. $^{13}\text{C}\{^1\text{H}\}$ NMR spectrum of **1** in $d_8\text{-THF}$.

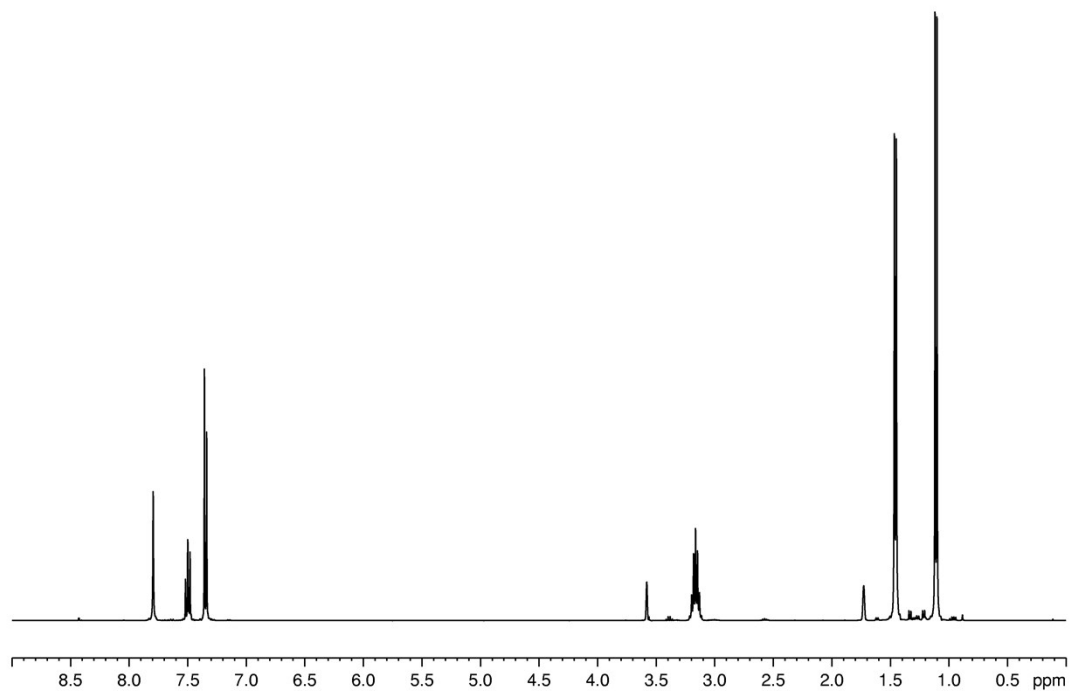


Figure S3. ^1H NMR spectrum of **2** in $d_8\text{-THF}$.

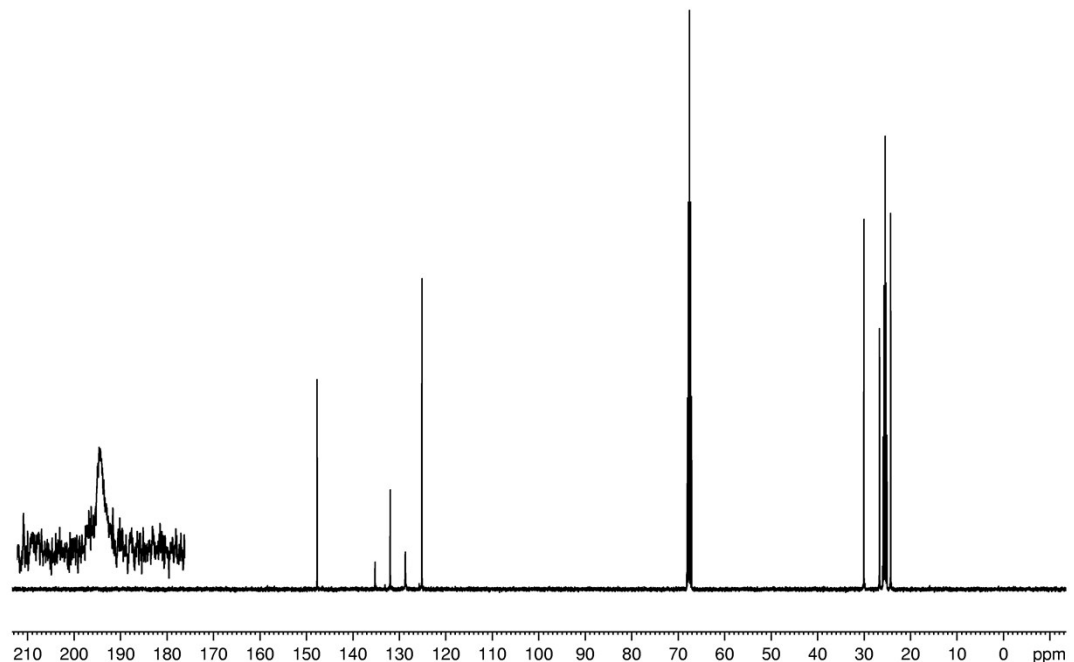


Figure S4. $^{13}\text{C}\{^1\text{H}\}$ NMR spectrum of **2** in $d_8\text{-THF}$.

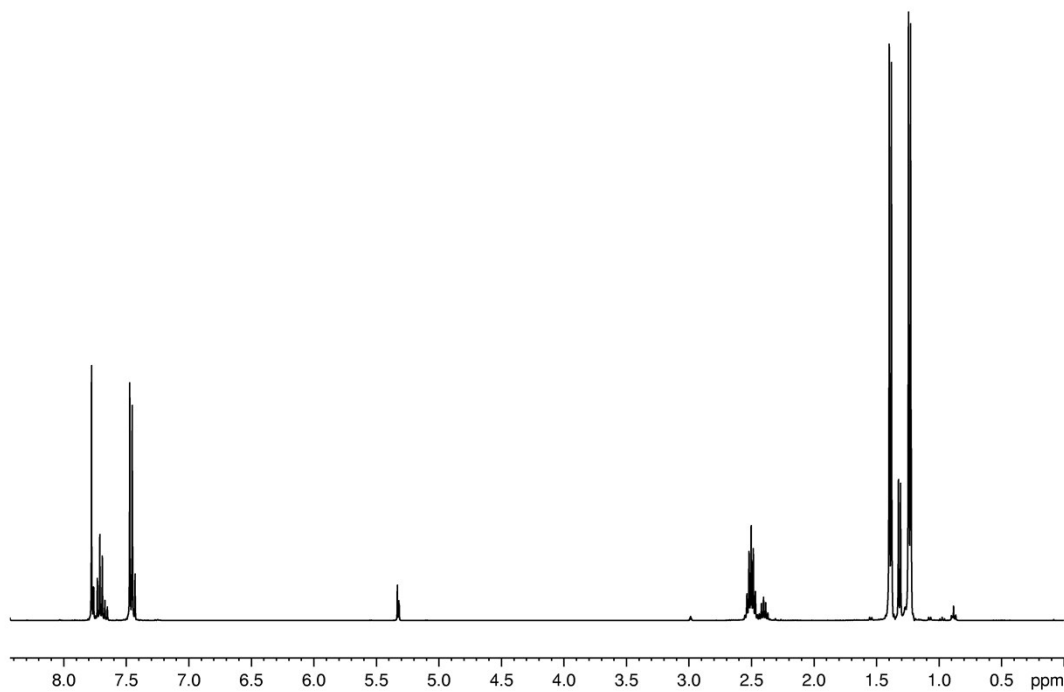


Figure S5. ¹H NMR spectrum of [3][AlBr₄] in CD₂Cl₂.

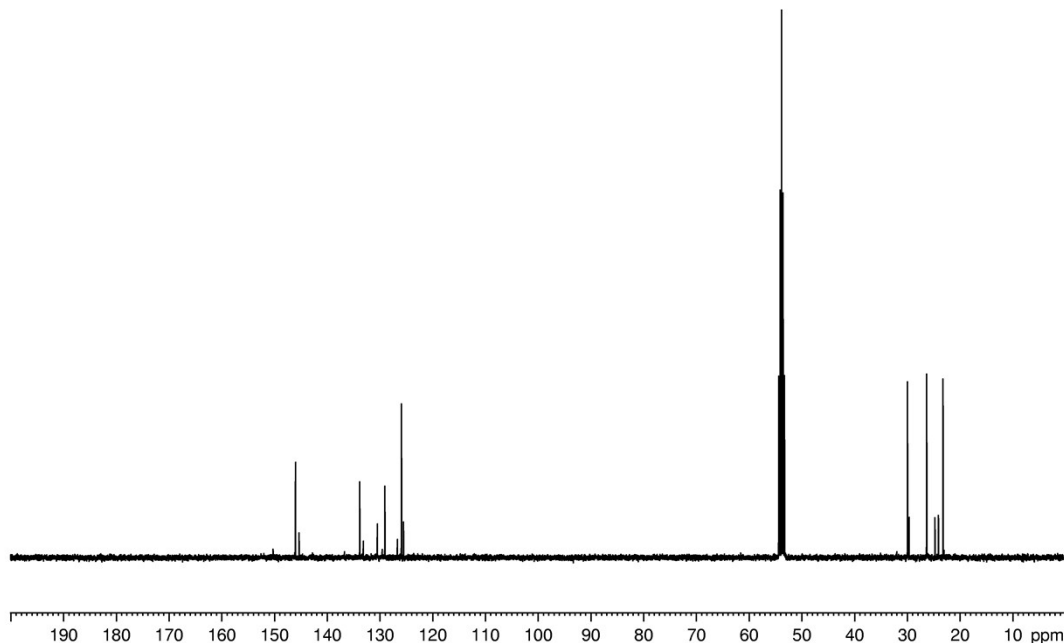


Figure S6. ¹³C{¹H} NMR spectrum of [3][AlBr₄] in CD₂Cl₂.

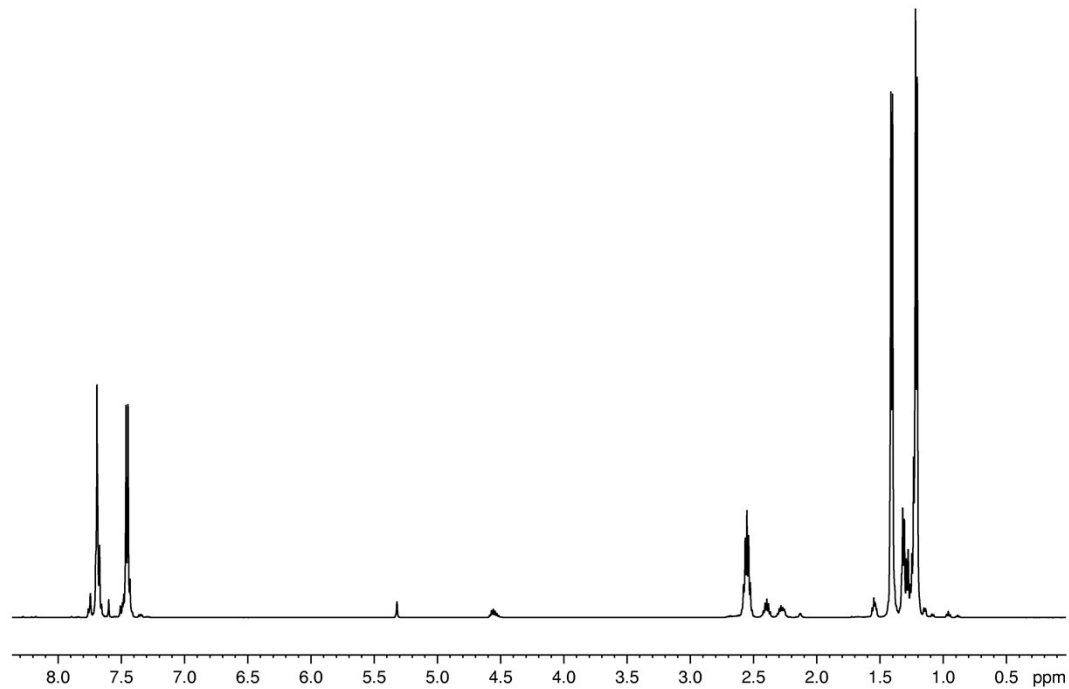


Figure S7. ¹H NMR spectrum of [4][AlBr₄] in CD₂Cl₂.

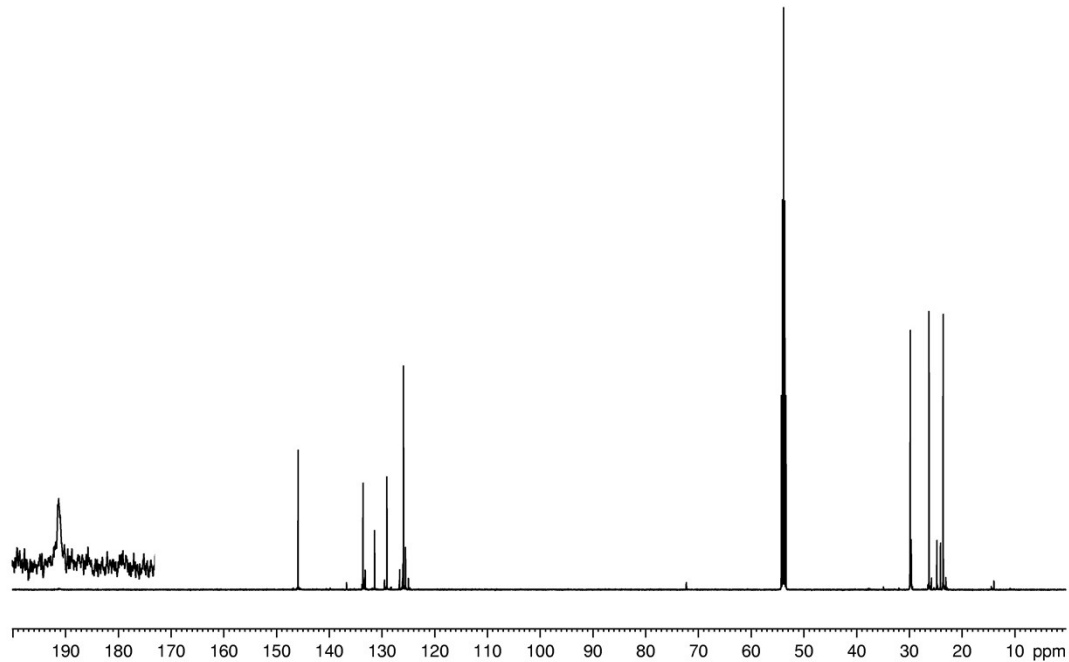


Figure S8. ¹³C{¹H} NMR spectrum of [4][AlBr₄] in CD₂Cl₂.

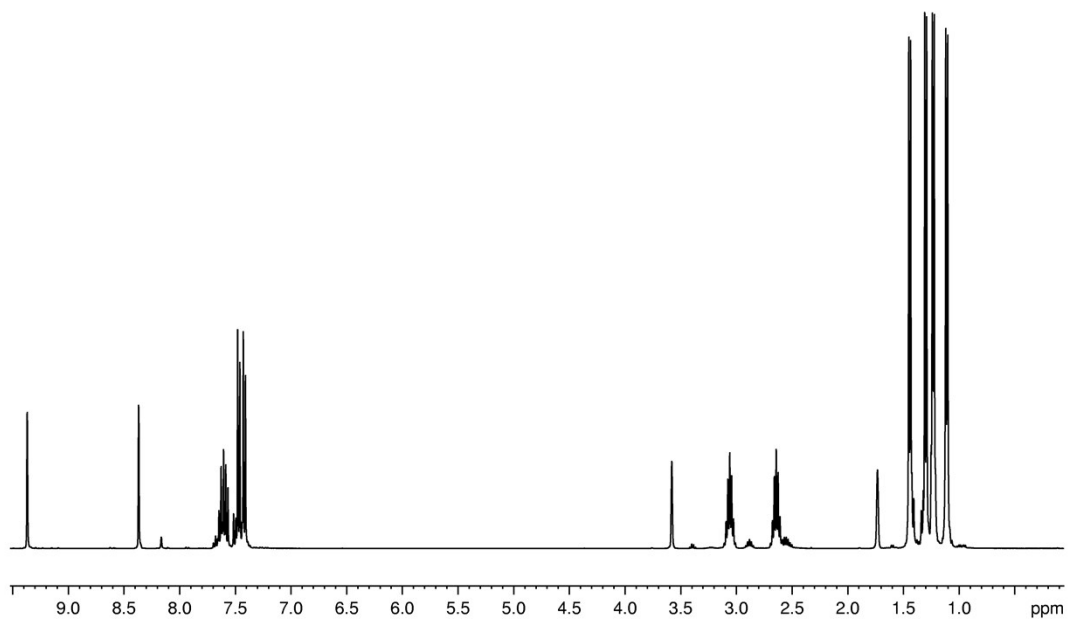


Figure S9. ^1H NMR spectrum of **5** in $d_8\text{-THF}$.

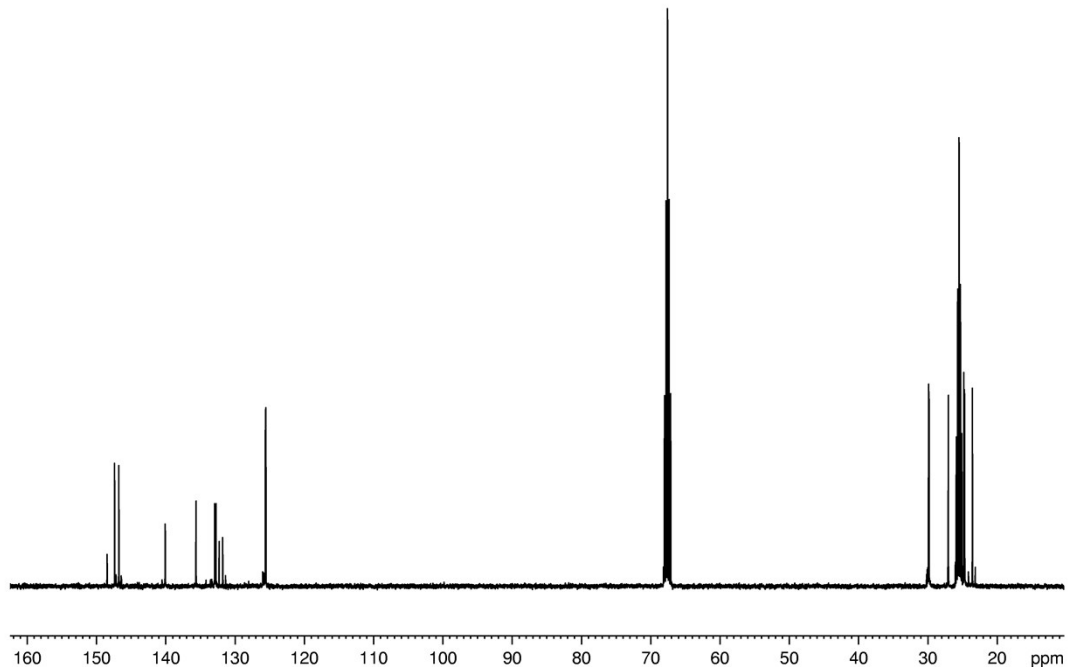


Figure S10. $^{13}\text{C}\{\text{H}\}$ NMR spectrum of **5** in $d_8\text{-THF}$.

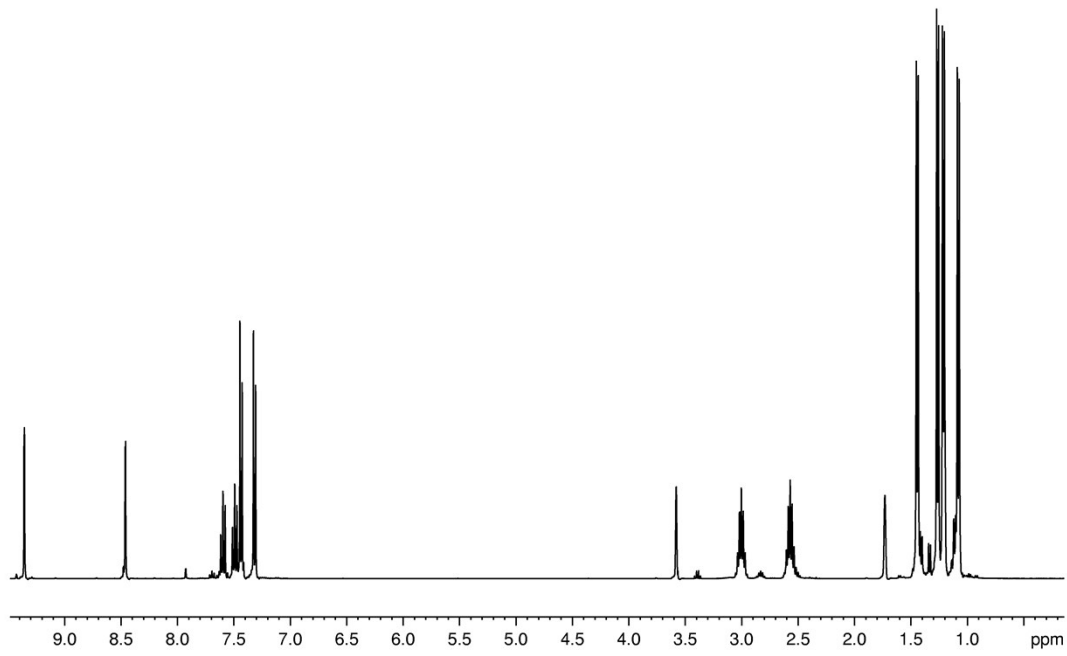


Figure S11. ^1H NMR spectrum of **6** in $d_8\text{-THF}$.

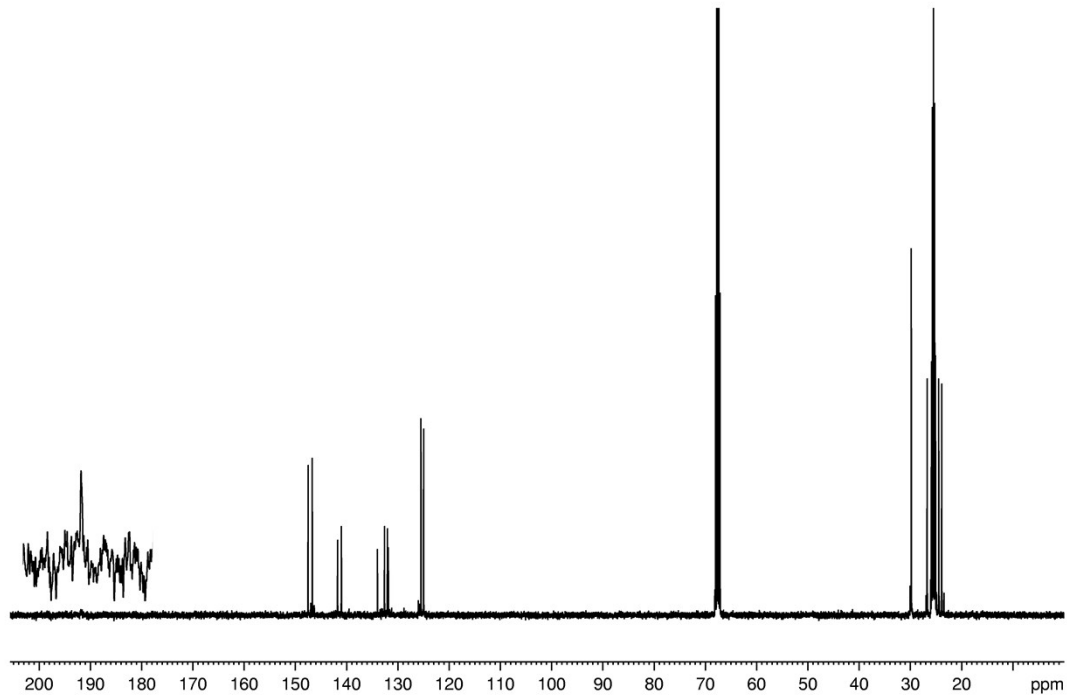


Figure S12. $^{13}\text{C}\{\text{H}\}$ NMR spectrum of **6** in $d_8\text{-THF}$.

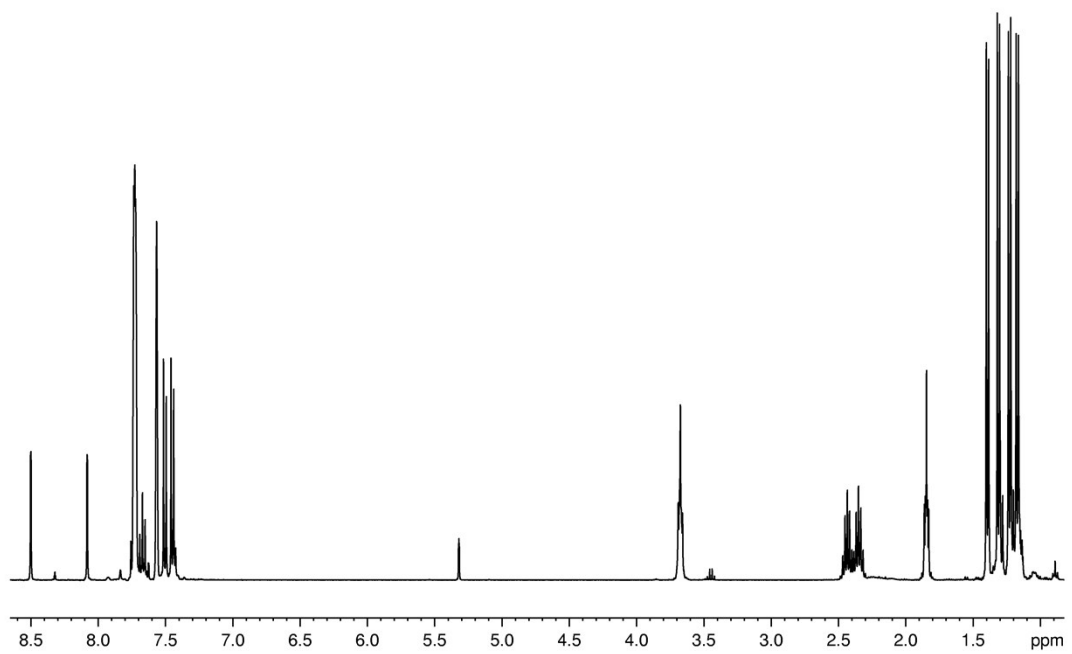


Figure S13. ¹H NMR spectrum of [7][BAr^F₄] in CD₂Cl₂.

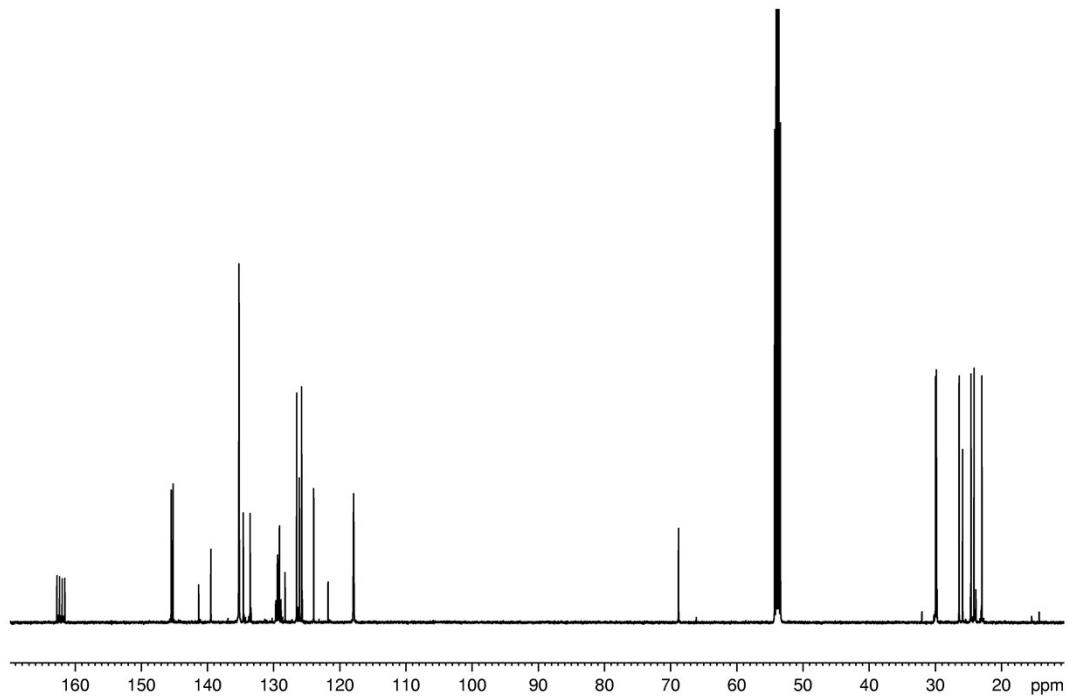


Figure S14. ¹³C{¹H} NMR spectrum of [7][BAr^F₄] in CD₂Cl₂.

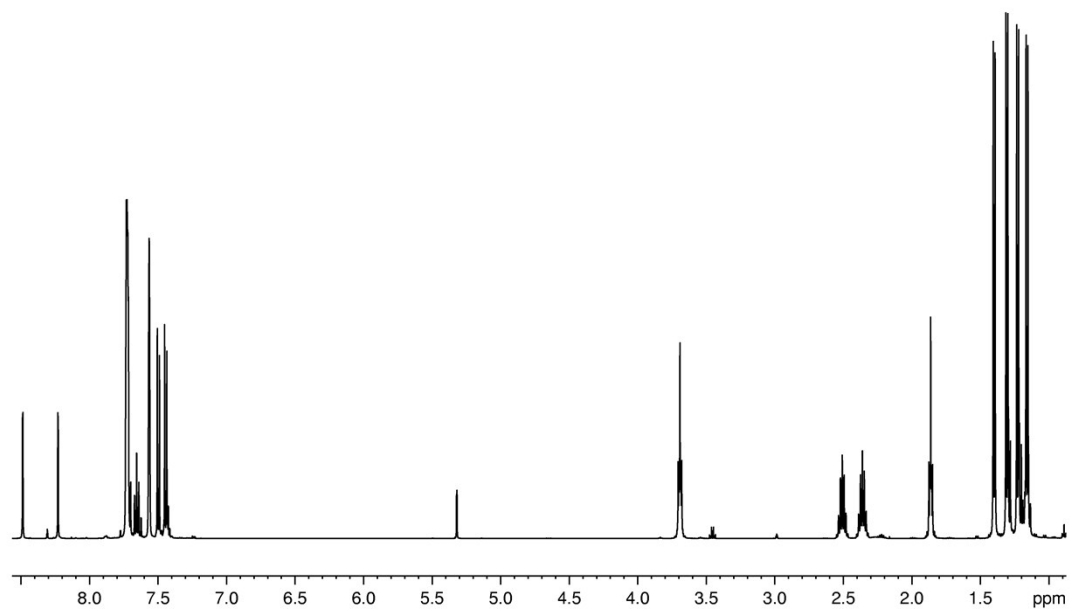


Figure S15. ¹H NMR spectrum of **[8][BArF₄]** in CD₂Cl₂.

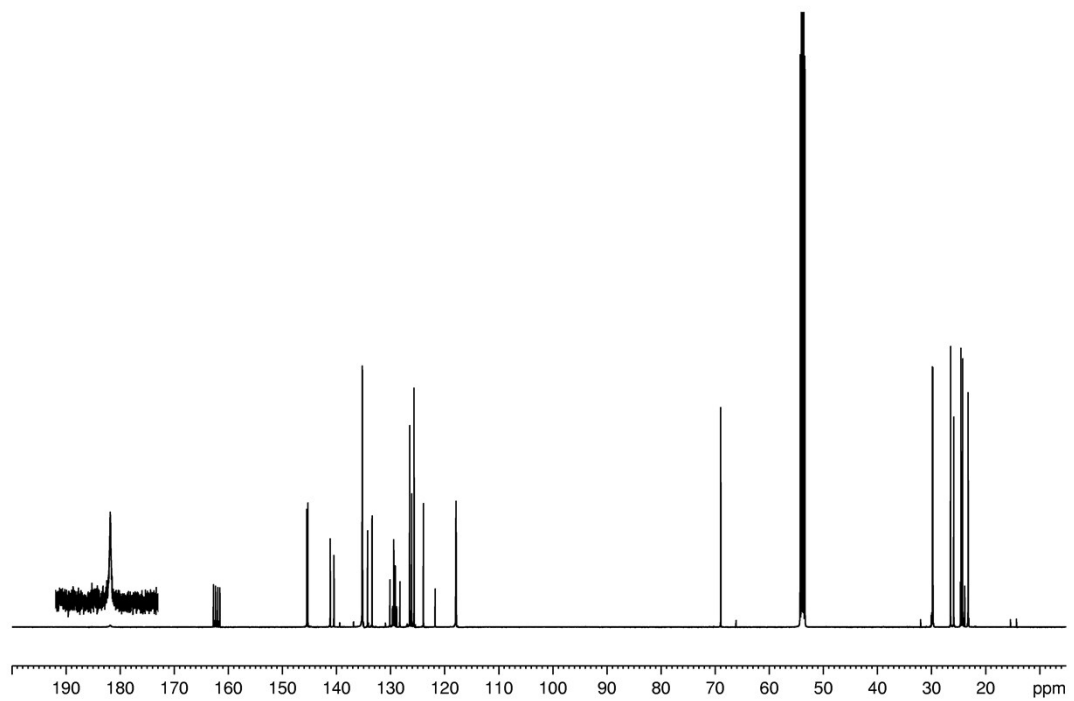


Figure S16. ¹³C{¹H} NMR spectrum of **[8][BArF₄]** in CD₂Cl₂.

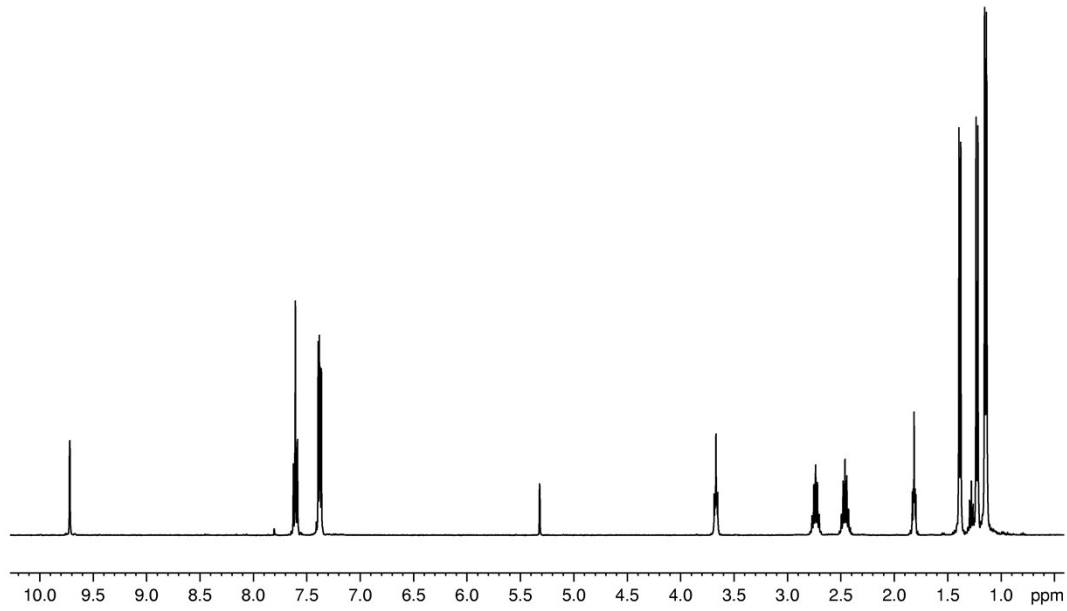


Figure S17. ¹H NMR spectrum of [9]Br in CD_2Cl_2 .

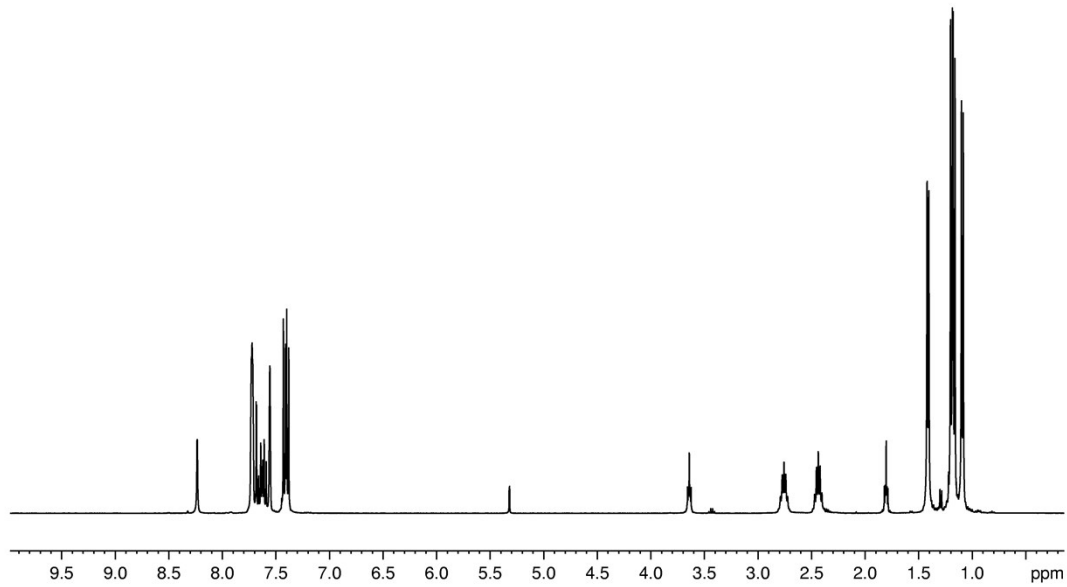


Figure S18. ¹H NMR spectrum of [9][BArF₄] in CD_2Cl_2 .

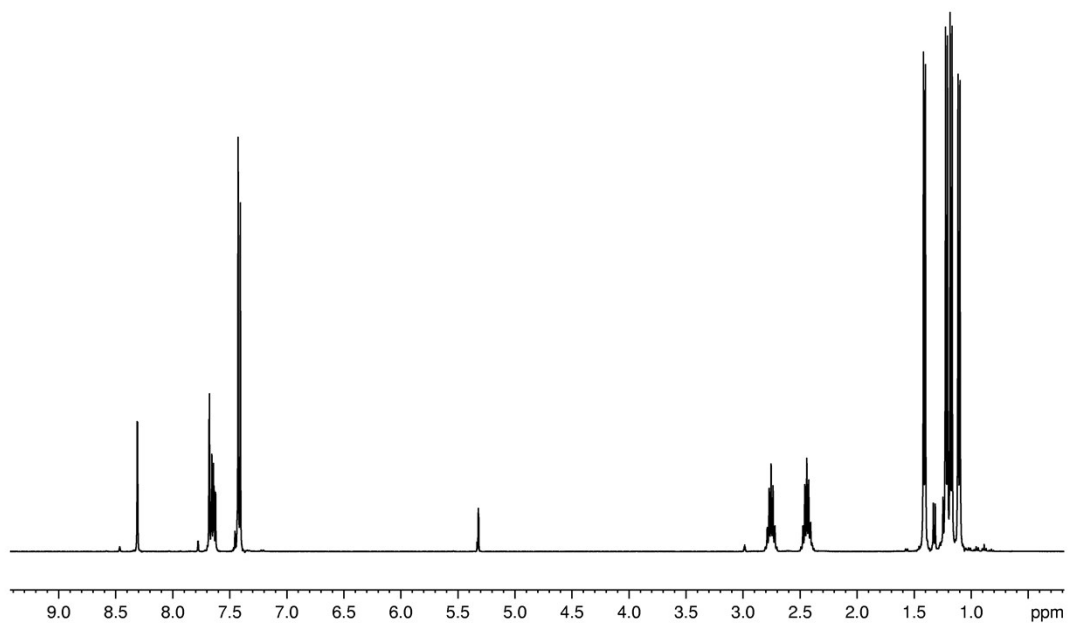


Figure S19. ^1H NMR spectrum of $[9]\text{[AlBr}_4]$ in CD_2Cl_2 .

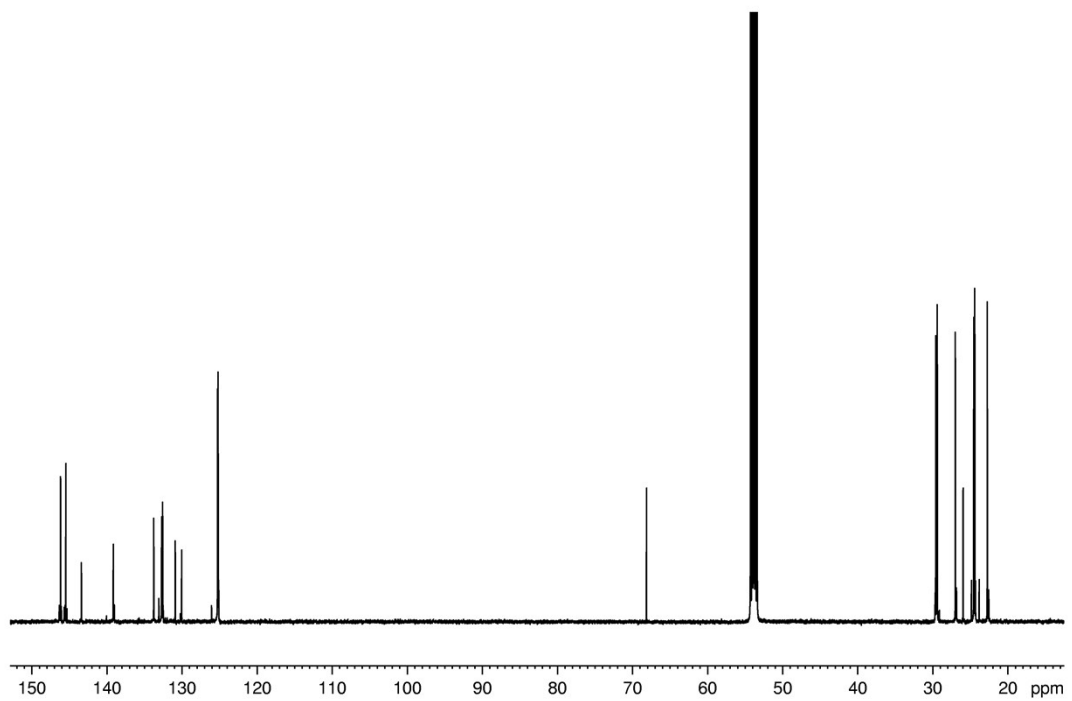


Figure S20. $^{13}\text{C}\{\text{H}\}$ NMR spectrum of $[9]\text{Br}$ in CD_2Cl_2 .

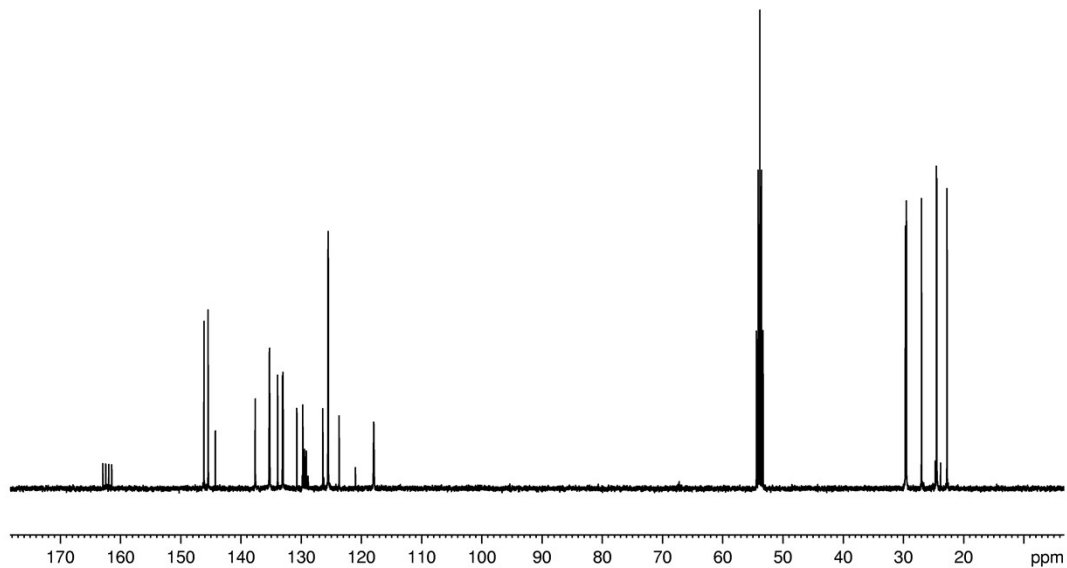


Figure S21. $^{13}\text{C}\{\text{H}\}$ NMR spectrum of **[9][BArF₄]** in CD_2Cl_2 .

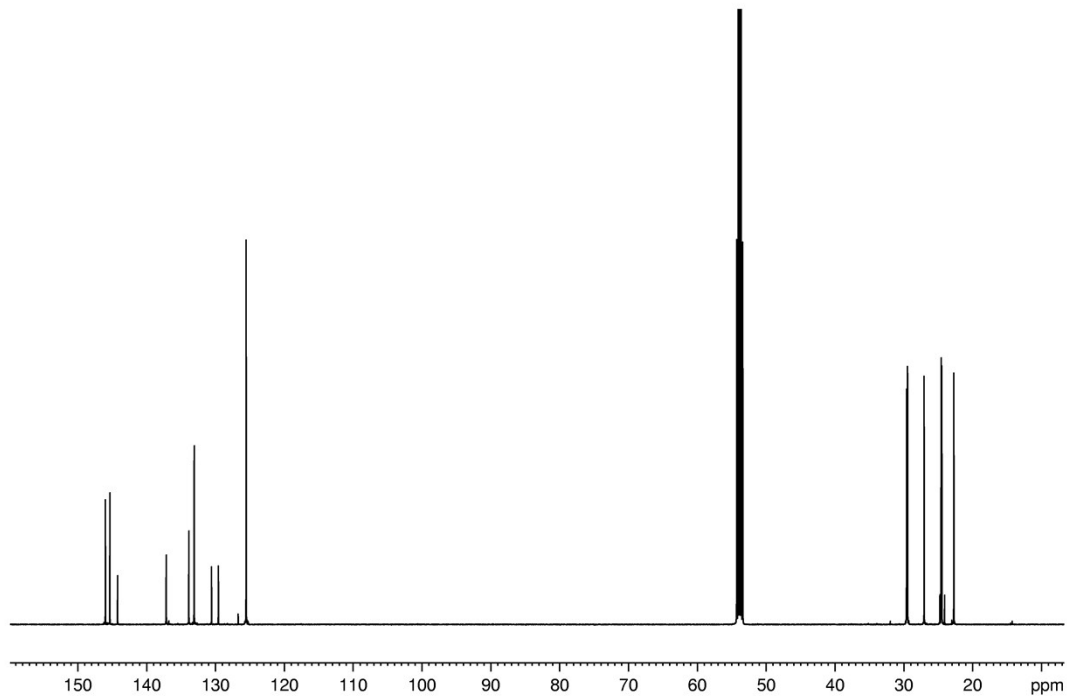


Figure S22. $^{13}\text{C}\{\text{H}\}$ NMR spectrum of **[9][AlBr₄]** in CD_2Cl_2 .

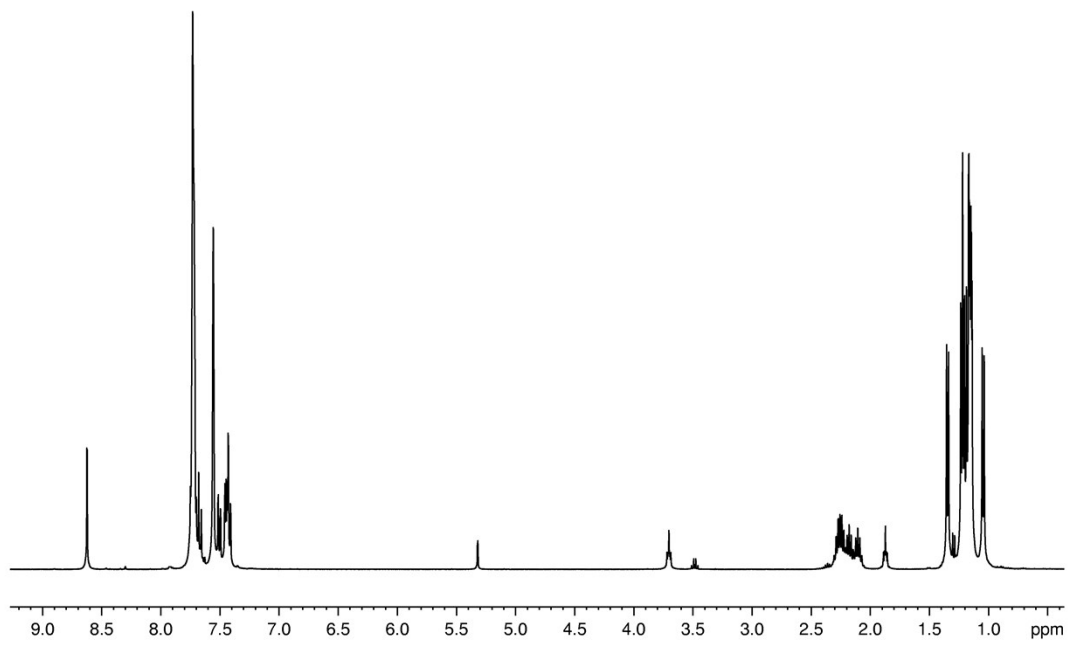


Figure S23. ¹H NMR spectrum of **[10][BArF₄]₂** in CD₂Cl₂.

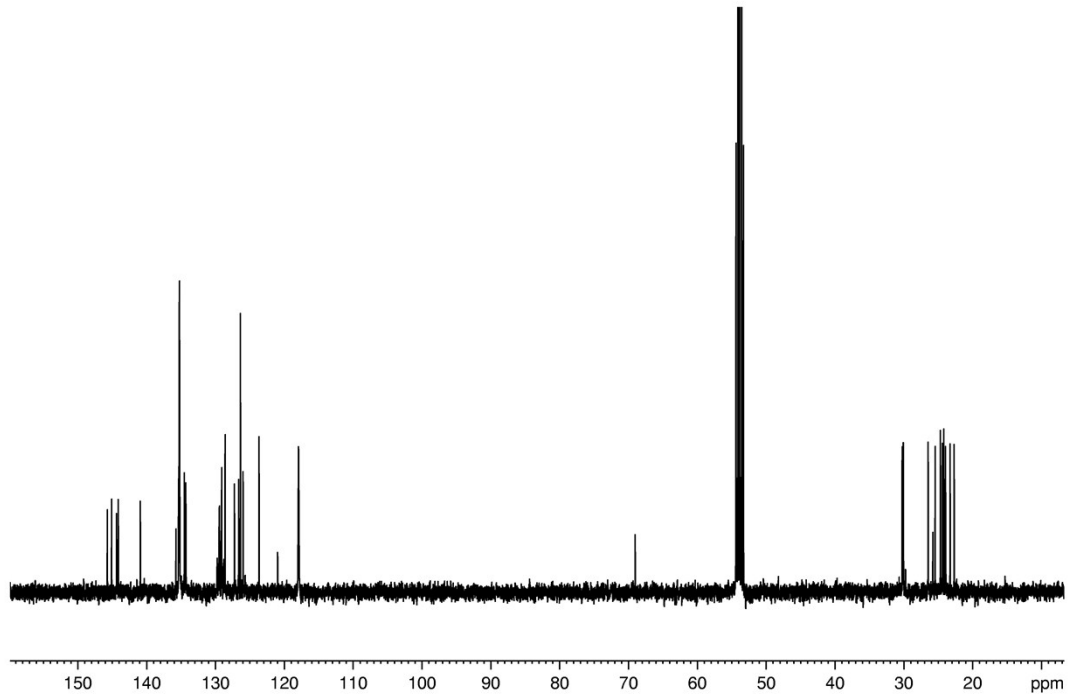


Figure S24. ¹³C{¹H} NMR spectrum of **[10][BArF₄]₂** in CD₂Cl₂.

3. ESI-MS spectra

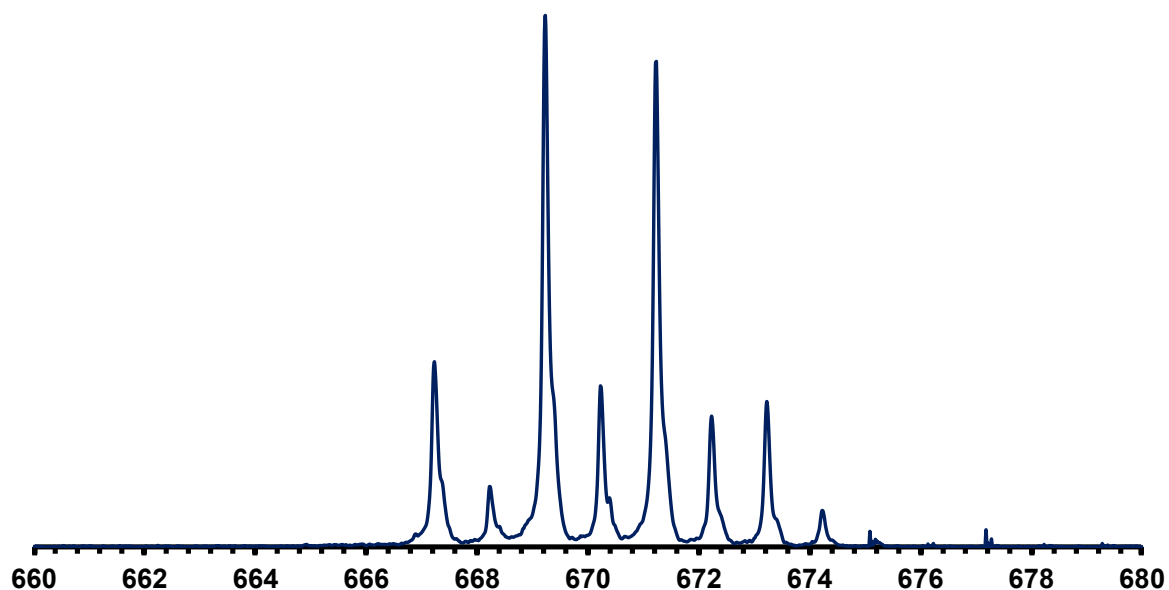


Figure S25. Mass envelope observed for **3** in the positive ion mode ESI-MS spectrum of $[3][\text{AlBr}_4]$.

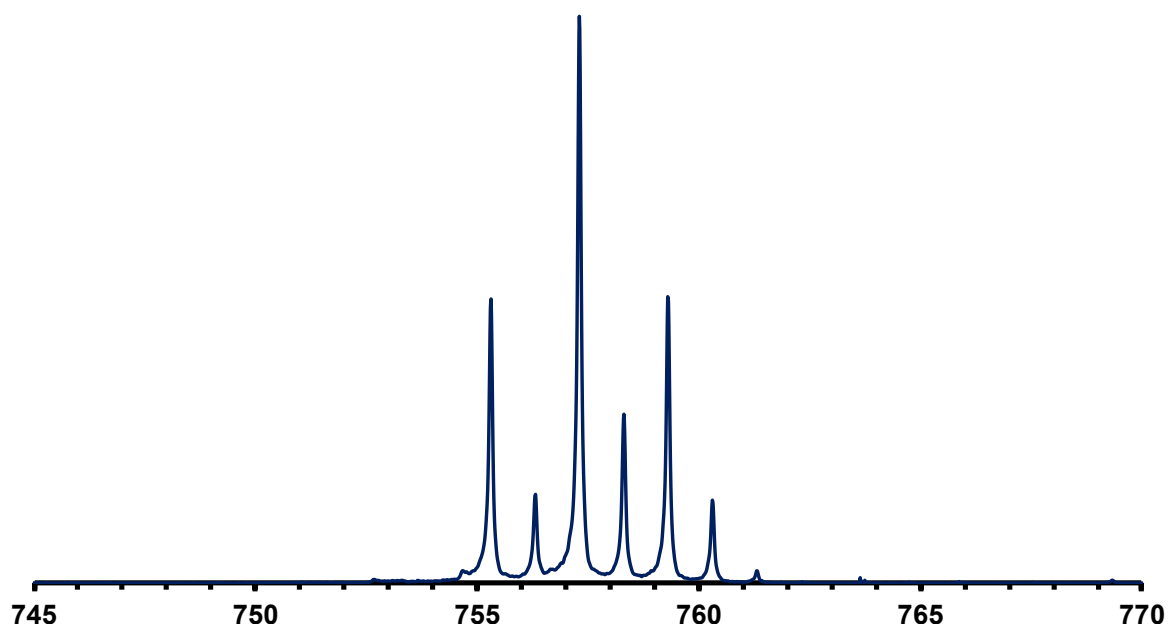


Figure S26. Mass envelope observed for **4** in the positive ion mode ESI-MS spectrum of $[4][\text{AlBr}_4]$.

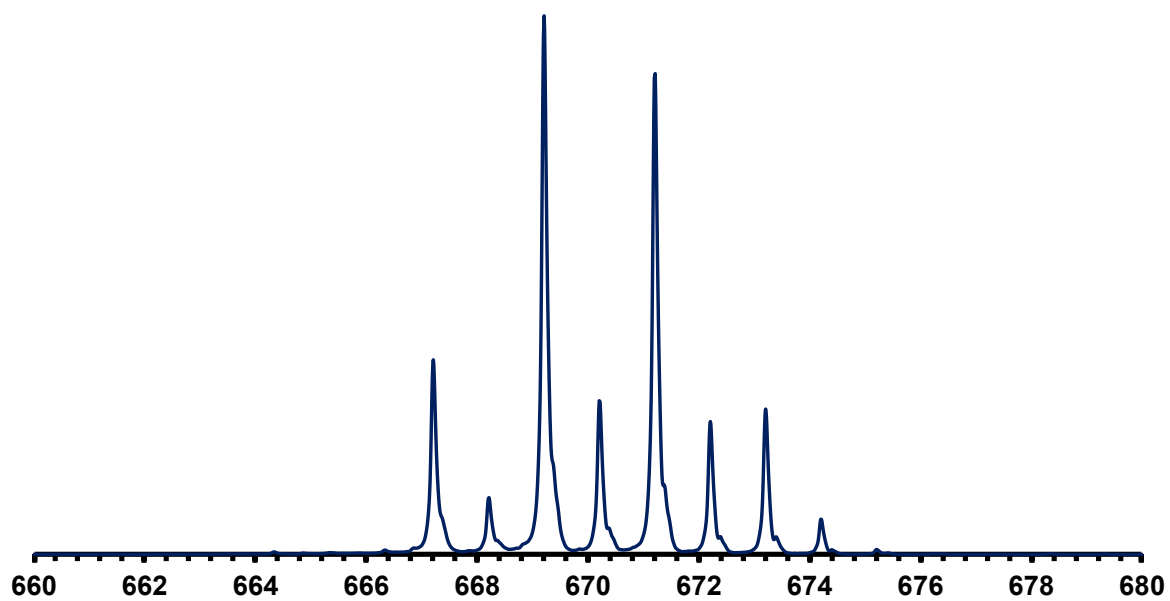


Figure S27. Mass envelope observed for **7** in the positive ion mode ESI-MS spectrum of $[7][\text{BArF}_4]$.

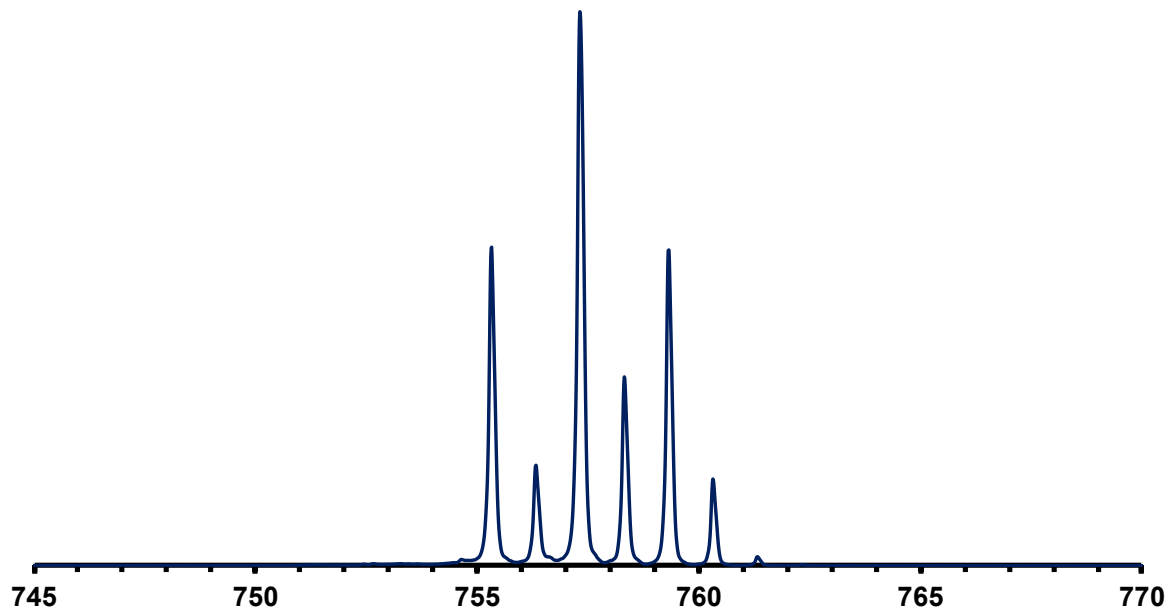


Figure S28. Mass envelope observed for **8** in the positive ion mode ESI-MS spectrum of $[8][\text{BArF}_4]$.

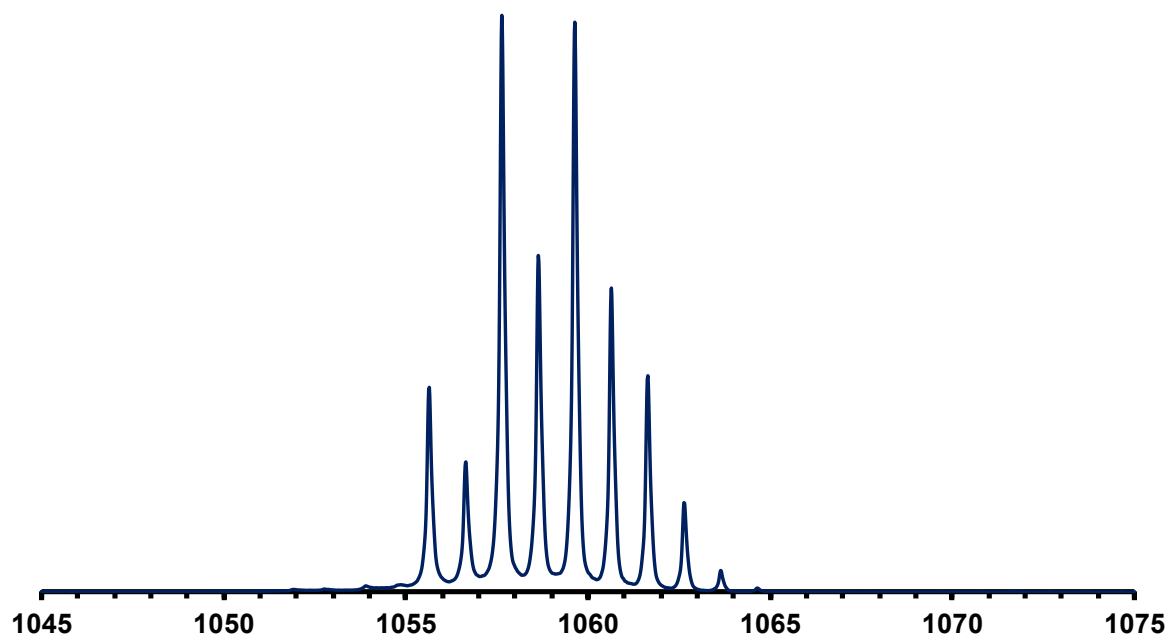


Figure S29. Mass envelope observed for **9** in the positive ion mode ESI-MS spectrum of $[9][\text{BAr}^{\text{F}}_4]$.

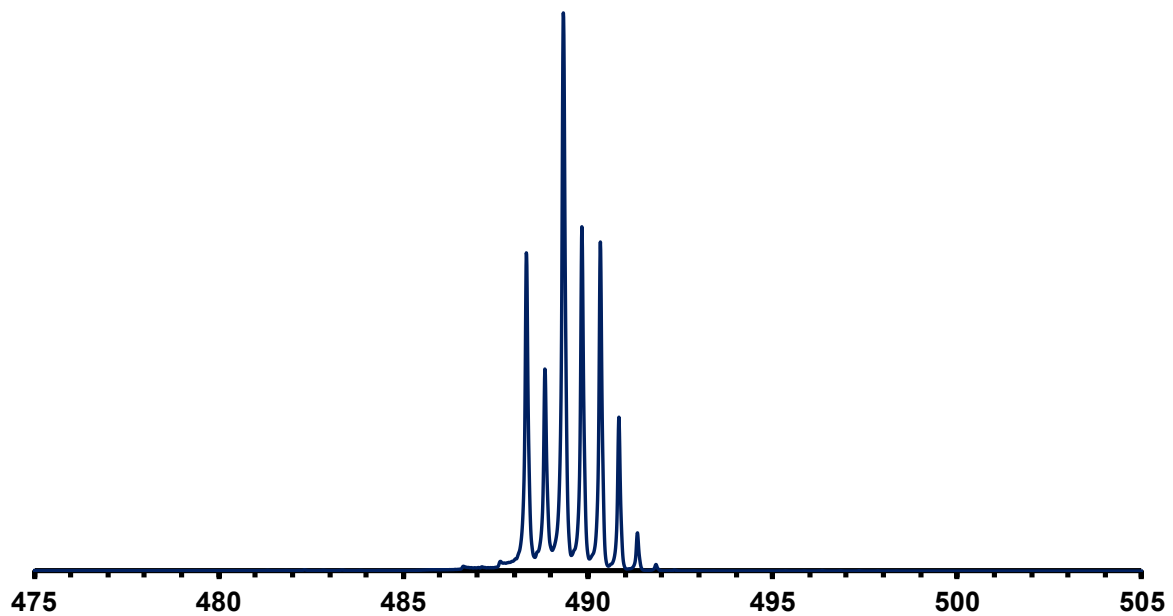


Figure S30. Mass envelope observed for **10** in the positive ion mode ESI-MS spectrum of $[10][\text{BAr}^{\text{F}}_4]_2$.

4. Computational details

DFT computations were performed using Gaussian 09, Revision D.01,^[1] implementing the hybrid functional PBE1PBE. 6-31G(d,p) basis sets were used for all atoms except Br, Sb and Bi for which the fully relativistic energy-consistent pseudopotentials (ECPs)^[2] were employed (ECP28MDF for Br, ECP46MDF for Sb and ECP78MDF for Bi), along with the corresponding basis set.^[3] Stationary points were confirmed to be minima by the absence of imaginary frequencies.

Compound	Total Energy (E_h)
(IPr)SbBr ₃ (1)	-1204.40114744
(IPr)BiBr ₃ (2)	-1204.44905838
[(IPr)BiBr ₃] ₂	-2408.91938598
[(IPr)BiBr ₃] ₂ (planar)	-2408.91895308
(aIPr)SbBr ₃ (5)	-1204.40490314
[(aIPr)SbBr ₃] ₂	-2408.84075052
(aIPr)BiBr ₃ (6)	-1204.44859133
[(aIPr)BiBr ₃] ₂	-2408.93166563
[(aIPr·2THF)SbBr ₂] ⁺ (7 ·2THF)	-1655.19966022
[(aIPr·2THF)BiBr ₂] ⁺ (8 ·2THF)	-1655.24512671
THF	-232.18530508
[(aIPr) ₂ SbBr ₂] ⁺ (9)	-2349.56172240
[(aIPr) ₂ SbBr ₂]Br ([9]Br)	-2363.13213460
[(aIPr) ₂ BiBr ₂] ⁺	-2349.58662421
[(aIPr) ₂ BiBr ₂]Br	-2363.15616954
Br ⁻	-13.46013171
IPr	-1158.68915469
[(aIPr) ₂ SbBr] ²⁺ (10)	-2335.86557689

References

- [1] Frisch, M. J.; Trucks, G. W.; Schlegel, H. B.; Scuseria, G. E.; Robb, M. A.; Cheeseman, J. R.; Scalmani, G.; Barone, V.; Petersson, G. A.; Nakatsuji, H.; Li, X.; Caricato, M.; Marenich, A.; Bloino, J.; Janesko, B. G.; Comperts, R.; Mennucci, B.; Hratchian, H. P.; Ortiz, J. V.; Izmaylov, A. F.; Sonnenberg, J. L.; Williams-Young, D.; Ding, F.; Lipparini, F.; Egidi, F.; Goings, J.; Peng, B.; Petrone, A.; Henderson, T.; Ranasinghe, D.; Zakrzewski, V. G.; Gao, J.; Rega, N.; Zheng, G.; Liang, W.; Hada, M.; Ehara, M.; Toyota, K.; Fukuda, R.; Hasegawa, J.; Ishida, M.; Nakajima, T.; Honda, Y.; Kitao, O.; Nakai, H.; Vreven, T.; Throssell, K.; Montgomery, Jr., J. A.; Peralta, J. E.; Ogliaro, F.; Bearpark, M.; Heyd, J. J.; Brothers, E.; Kudin, K. N.; Staroverov, V. N.; Keith, T.; Kobayashi, R.; Normand, J.; Raghavachari, K.; Rendell, A.; Burant, J. C.; Iyengar, S. S.; Tomasi, J.; Cossi, M.; Millam, J. M.; Klene, M.; Adamo, C.; Cammi, R.; Ochterski, J. W.; Martin, R. L.; Morokuma, K.; Farkas, O.; Foresman, J. B.; Fox, D. J. *Gaussian 09, Revision D.01, 2009*.
- [2] Stoll, H.; Metz, B.; Dolg, M. *J. Comput. Chem.* **2002**, *23* (8), 767–778.
- [3] Burkatzki, M.; Filippi, C.; Dolg, M. *J. Chem. Phys.* **2007**, *126* (23), 234105.